Journal of Electronic Materials, Vol. 15, No. 6, 1986

Equilibrium Solidification of Sn-Ag-Sb Thermal Fatigue-Resistant Solder Alloys

D. BRUCE MASSON

Professor
Washington State University
Pullman, Washington 99164

BRIAN K. KIRKPATRICK

RCA Sharp Microelectronics
P. O. Box 1044
Camas, Washington 98607

A survey of the liquidus surface and invariant reactions involving liquid has been made for solidification in the ternary Sn-Ag-Sb system. Differential thermal analysis and electron-beam microprobe analysis were used to measure liquidus temperatures and determine the composition of solid phases resulting from solidification. A liquidus projection and the composition of the phases coexisting at the two observed invariant reactions were determined. Ternary alloys based on the Sn-Ag-Sb system have been used as thermal fatigue-resistant solders where high heat loads must be dissipated. An analysis of the properties encountered from such solders is presented, based on the phase constitution resulting from the solidification behavior reported here.

Key words: Sn-Ag-Sb liquidus projection, solder alloys, Sn-Ag-Sb solders.

INTRODUCTION

The use of high-strength solders based on ternary alloys found in the tin-rich corner of the Sn-Ag-Sb system has attracted attention in cases where thermal fatigue is a problem. In these applications silicon chips are bonded to metallic substrates in which high heat loads may be dissipated. Such solders have the high tensile strength and low ductility that can be associated with resistance to thermal fatigue and to the resultant degradation of heat transfer during power cycles.

One alloy of this type which has been awarded a patent[1] because of its unique wetting and thermal fatigue resistance is alloy *J*, which contains 65% (by weight) tin, 25% silver and 10% antimony. The development of alloy *J* has been conducted without knowledge of equilibrium solidification temperatures or the phase distribution expected in this ternary system. While it has been recognized that large temperature differences can be expected in these alloys between the onset of solidification and final freezing, no information on the ternary liquidus surface appears in the literature. A study of the distribution of phases at low temperature has been made by Cheng,[2] although he did not investigate equilibria involving liquid. Since the onset of solidification and the phase distribution expected from freezing of liquid are central to behavior of solders, an investigation of the nature of the liquidus surface in the ternary Sn-Ag-Sb alloys seems appropriate.

We report here a preliminary survey of the main features of the liquidus surface. We have given special attention to identification of the four-phase invariant reactions involving liquid and to a determination of the composition of the solid phases partaking in these reactions. The results can be used to generate an outline of the liquidus surface and the composition of the phases coexisting in the two invariant equilibria. Although a detailed determination of isothermal contours on the liquidus surface was not made, sufficient information about the initiation and completion of freezing was obtained to be of considerable use in the analysis of Sn-Ag-Sb solders.

EXPERIMENTAL TECHNIQUE

The data collected during solidification were thermal arrests that could be used to determine the onset of primary, secondary and tertiary solidification, and chemical analyses of the solid phases with an electron-beam microprobe. Metallographic examination of the microstructures was used to identify the solid phases, and, especially, to identify the phase produced by primary freezing. Composition of the liquid at the invariant points as determined by altering the composition of the liquid of the specimens in a systematic fashion until only a single thermal arrest at the temperature of the invariant reaction was observed.

The specimens were made from pure metals of 99.99% nominal purity obtained from Cominco Electronic Materials of Spokane, Washington. Predetermined quantities of each metal were weighed to an accuracy of 0.05 gram to obtain approximately 100 grams of a specimen of known compo-

We wish to acknowledge the contribution of pure metals used in this research, as well as support and advice, by Cominco Electronic Materials of Spokane, Washington.

(Received March 24, 1986; revised July 28, 1986)

sition. To minimize oxidation and loss of the more volatile antimony, the tin and silver were melted first. Melting was carried out under argon in a graphite crucible made from grade 780GL graphite obtained from AIRCO, Inc. The interior of the crucible was a cylindrical cavity 75 mm long and 25 mm i.d. The argon atmosphere was maintained during melting by directing a stream of argon into the cavity, which was approximately half-filled with the specimen and half with argon. The antimony was added when the tin and silver had melted and the temperature was estimated to be 50 to 100 degrees above the liquidus temperature. The liquid was stirred vigorously with a graphite rod; it was then allowed to solidify around a graphite sleeve into which the thermocouple for thermal analysis could be inserted. No loss of antimony vapor was detected visually during melting, and the oxide-free surface obtained after solidification was used as an indication that metal loss during melting had been minimal. No bulk chemical analyses were made after melting.

Thermal arrests were made by differential thermal analysis of these specimens. They were contained in the graphite melting crucibles, which in turn, were held within a closed silica tube in a furnace. The silica tube was evacuated and backfilled with argon before the specimens were melted at the start of the thermal analysis. The reference for the differential analysis was a cylindrical rod of nickel which had roughly the same heat capacity as the specimen. Chromel-alumel thermocouples were used; they were calibrated with pure metals at the melting point of tin (231.97° C), cadmium (321.11° C), zinc (419.58° C) and aluminum (660.37° C).

During thermal analysis a cooling rate of approximately 1 1/2 °C/min was maintained. The dc millivolt signal from the differential thermocouple was stored at 30 second intervals in a HP3497A Data Acquisition/Control Unit, which itself was controlled by a HP87XM computer. The millivolt data were converted to temperature, T, and differential temperature, θ, and graphed in a HP9872C Plotter, most importantly as curves of derived inverse differential, $d\theta/dT$, vs. temperature. Thermal arrests were prominent on these graphs and could easily be resolved from the background, since in many instances $d\theta/dT$ tends to infinity as a latent heat is evolved.

Initial identification of solid phases resulting from freezing of each specimen was made from chemical analysis with a Cameca MBX electron-beam microprobe. All phases present were found to be those which appear in one of the three binary systems—there appear to be no true ternary intermediate phases. After the initial identification, the phases could be recognized by their microstructural appearance in specimens etched with an etchant containing 100 ml glycerol, 9 ml nitric acid and 9 ml glacial acetic acid.

Once a rough idea of the nature of the liquidus surface was obtained from the primary thermal arrests, consideration was given to determination of the composition of the liquid participating in the four-phase invariant reactions. The temperature of invariant reactions is easily identified because a thermal arrest at this temperature appears in the cooling curves of several different specimens. We made an initial estimate of the composition of the liquid that freezes at each invariant point, and obtained a thermal arrest curve of a liquid made to have this estimated composition. Thermal arrest curves from the first estimates showed secondary peaks because we did not correctly guess the invariant composition. We then adjusted the composition until the thermal arrest curve revealed only a primary peak at the (previously-determined) temperature of the invariant reaction. This is believed to indicate that the liquid had been correctly made up to the invariant composition.

Composition of the solid phases resulting from invariant freezing is also difficult to measure because failure to attain equilibrium during freezing is characteristic of this system. Since each solid phase can appear to have several analyses, depending where the microprobe beam strikes, it is difficult to know which location was in equilibrium with the invariant liquid. In an attempt to attain equilibrium, specimens were held for 32 days in evacuated silica capsules at a temperature just below the invariant temperature (a 224° C anneal for the invariant at 235° C, a 364° C anneal for the invariant at 378° C). Composition of the phases present was determined with the microprobe after these anneals. This was only partially successful in revealing the equilibrium composition because solidification over a range of temperature had produced a corresponding range of composition for the solid phases. This range was not completely eliminated by long holding. In addition, partial melting of one specimen was encountered due to the unexpected presence of nonequilibrium liquid. Nevertheless, the compositions given in Table II are our best estimates. These compositions are also consistent with corresponding binary invariant points readily available from phase diagrams published in the ASM Handbook.[3]

DATA AND RESULTS

The composition of the twenty-one mixtures studied and the temperature of the thermal arrests are shown in Table I. The first-listed thermal arrest temperature is the liquidus temperature observed; a three dimensional plotting of these should comprise the liquidus surface. Our estimate from these data of the appearance of the liquidus projection is shown in Fig. 1. The second listed thermal arrest is that of secondary solidification, showing the onset of simultaneous freezing of two solid phases. These points should fall on the liquidus valleys of Fig. 1, which are lines at which surfaces of primary solidification intersect. The composition of the liquid at the onset of secondary freezing is not known, however, so the intersection of the liquidus surfaces cannot be determined from secondary thermal ar-

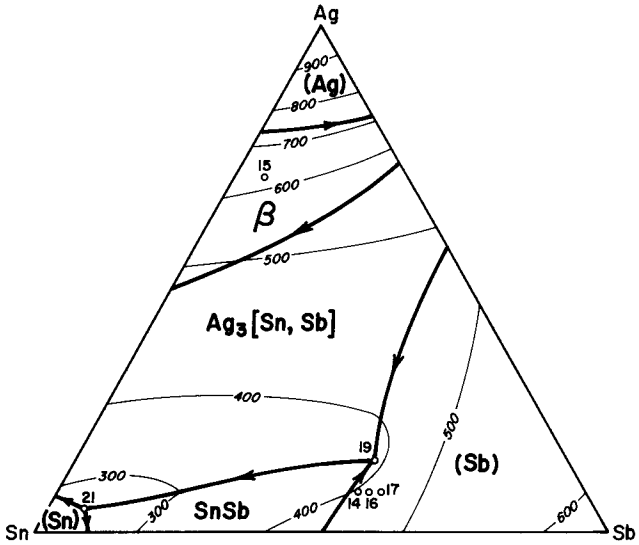

Fig. 1 — Liquidus projection of the Sn-Ag-Sb system. Points marked 14–17 show specimen compositions for which the liquid does not continue to follow a liquidus valley during secondary solidification.

rests. The points marking the composition of the primary phase, the bulk composition of the specimen and the composition of this secondary liquid should be colinear; this is sometimes of assistance in locating the liquidus valleys.

The method of ascertaining the composition of the liquid at the invariant reactions—seeking a liquid with a single thermal arrest at the correct temperature—has been mentioned previously. The specimens showing this behavior are numbered 19 and 21. The average value of the invariant temperatures are 378.5° C and 234.8° C.

Table II. Composition of Phases at Invariant Temperature

Invariant Reaction	Phase	Composition Sn	Ag	Sb
$L + (Sb) \rightleftharpoons Ag_3[Sn,Sb] + SbSn$	Liquid	34	14	52
378.5° C	(Sb)	11	0*	89
	$Ag_3[Sn,Sb]$	18	72	10
	SbSn	36	0*	64
$L + SbSn \rightleftharpoons Ag_3[Sn,Sb] + (Sn)$	Liquid	89	5	6
234.8° C	SbSn	57	0*	43
	$Ag_3[Sn,Sb]$	27	72	1
	(Sn)	92	0*	8

*Solubility of silver is less than 1% in alloys on the Sn-Sb side. Percentages of silver above background in the microprobe analyses are as follows: (Sn) 0.1% SbSn 0.0% with Sn (Sb) 0.0% SbSn 0.2% with Sb

The liquidus surface suggested here is consistent with our identification of primary microconstituents with both the microprobe and metallographic examination, and with the thermal arrests. The composition of the solid phases which are in equilibrium at the invariant temperature was deduced from microprobe analyses of the specimens held for 32 days at a temperature just below the invariant temperature. These compositions are listed in Table II. It is clear that the terminal (Sn) and (Sb) solutions, and the intermetallic compound SbSn have very limited solubility for silver. The solubility of antimony in the (Sn) and SbSn, and that of tin in (Sb), are close to the values shown in the binary Sb-Sn system.

Table I. Specimen Composition and Temperature of Thermal Arrests

Sample No.	Composition, wt. % Sn	Ag	Sb	Thermal Arrest Temperature, °C Primary	Secondary	Other	Invariant
1	40	20	40	380.8			235.5
2	80	10	10	247.0			235.0
3	45	45	10	488.1	302.1		236.4
4	80	5	15	287.9			235.3
5	30	10	60	480.1			376.9
6	10	30	60	517.1	455.4		378.4
7	10	55	35	486.3	443.0		378.2
8	25	31	44	423.5			378.5
9	44	8	48	398.7	362.9		234.4
10	44	8	48	399.0	362.9		234.3
11	42	8	50	423.8	396.8	369.2 364.7	234.3
12	10	85	5	810.6	715.7		
13	15	70	15	598.5	523.3		379.5
14	40	8	52	430.5	394.8	370.0	234.6
15	25	70	5	614.7	493.9		233.5
16	38	8	54	447.8	393.0	370.9	234.4
17	36	8	56	462.9	390.6	372.1	234.1
18	15	40	45	463.3	447.7		379.0
19	34	14	52				379.1 234.3
20	83	8	9	251.0			235.2
21	89	5	6				235.1

DISCUSSION

The location of the point representing composition of the invariant liquid appears as expected from a ternary reaction of the type called Class II by Rhines.[4] In such a class the complete peritectic plane is a four-sided trapezium with composition of each of the coexisting phases appearing at one corner. The nominal equations for the invariant reactions are

Eqn. 1 $(Sb) + L \rightleftharpoons SbSn + Ag_3[Sb,Sn]$
Eqn. 2 $SbSn + L \rightleftharpoons (Sn) + Ag_3[Sb,Sn]$

378.5° C
234.8° C

On a liquidus surface it is common for a Class II reaction to occur if two liquidus valleys descend from higher temperatures, intersect, and a single valley decends (in temperature) from the intersection. The results of Cheng[2] and the microprobe analyses suggest that the phase field and liquidus surface of the γ phase, $Ag_3[Sn,Sb]$, is continuous across the diagram from the Ag-Sn side to the Ag-Sb side. Cheng's measurements also indicate that the phase β, Ag(Sn,Sb), is continuous, as we have shown here.

The tendency for non-equilibrium freezing in this system is great. It is apparent from Table I that a number of specimens show a thermal arrest at both 234.8° and 378.5°, or that some show an arrest at 234.8° even though the point representing the composition does not fall on the peritectic plane. If equilibrium were followed, neither occurrence should be observed. Alloy 19, for example, should solidify completely at a temperature not far below 378° and should not have liquid remaining at 235° (as it does). This non-equilibrium aspect of solidification is probably a result of the Class II reactions producing a peritectic-type of envelopment.

Another feature of this ternary system is the tendency of the liquid during solidification to "leave" the liquidus valley and move across a new liquidus surface. Although this is not a common phenomenon in solidification of metals, it can be illustrated here by specimen 15. This specimen begins primary freezing of β at 615° C, and secondary freezing of β and $Ag_3[Sn,Sb]$ at 493° C. At a temperature below the onset of secondary freezing, the liquid becomes too poor in silver to continue solidifying to both β and $Ag_3[Sn,Sb]$. The liquid then "leaves" the liquidus valley, now freezing only $Ag_3[Sn,Sb]$, and travels across the $Ag_3[Sn,Sb]$ surface. At equilibrium there is liquid remaining at a temperature as low as 235° C, which is the temperature of final freezing. This is an equilibrium characteristic, but it causes such a mixture to show a large range in temperature between the onset and completion of freezing. Such a departure of liquid from the liquidus valley also occurs in specimens 14, 16 and 17. Here the effect on the freezing range is less dramatic, but the effect causes more thermal arrests than might normally be expected.

In the study of Sn-Ag-Sb solders, Olsen and Spanjer[1,5] sought a solder of high tensile strength and low ductility, a combination which appears to ensure freedom from thermal fatigue. They have published[1,5] results of mechanical testing of twelve alloys studied in their development program. The interpretation of their results is made somewhat easier by an analysis based on Fig. 2. It seems apparent, for example, that the strength of the alloy is strongly influenced by the strength of the tin-rich terminal solid solution, (Sn). Tin dissolves very little silver, but can dissolve up to 9% or 10% antimony. Attaining maximum strength appears to depend on saturating the (Sn) phase with antimony—this will occur if the composition falls within the 3-phase Sn + SnSb + $Ag_3[Sn,Sb]$ triangle. The effect of saturation can be seen in the tensile strength of alloys, E, G and L studied by Olsen and Spanjer.[1,5] All three of these alloys have 20% silver, so have equal amounts of the silver-rich $Ag_3[Sn,Sb]$ phase, but the antimony has been increased from 1.5% to 5% to 10% from E to L. Only their alloy L has enough antimony to saturate the (Sn)—this is consistent with the progression of tensile strength in these three from 56.1 to 78.1 to 91.1 MPa. On the other hand, alloys J, K, and L all fall within the 3-phase triangle, all consequently have (Sn) saturated with antimony, and all have strengths in excess of 90 MPa.

A second effect on tensile strength is apparently caused by the amount of silver-rich $Ag_3[Sn,Sb]$ present in those alloys in which (Sn) is saturated. By using the lever rule it can be seen that the highest strength occurs when the (Sn) phase is saturated with antimony and the amount of $Ag_3[Sn,Sb]$ is at a maximum.

Low ductility is associated with presence of SbSn, undoubtedly a brittle intermetallic compound. Alloys J, K and L exhibit this; the lowest ductility

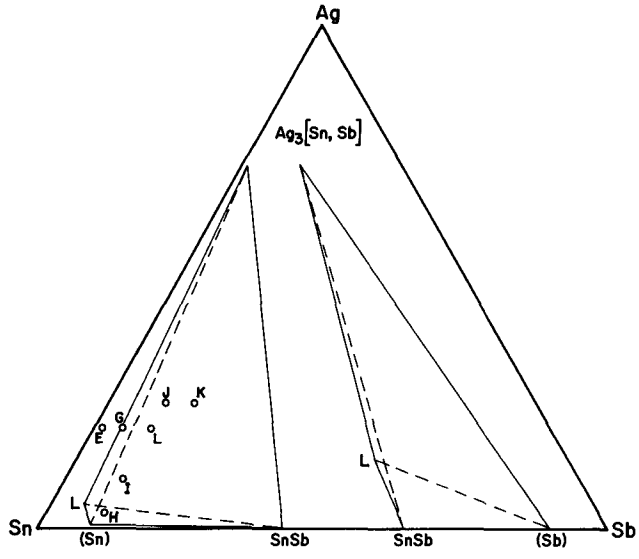

Fig. 2 — Composition of co-existing phases for the two invariant reactions in Sn-Ag-Sb. Points marked E–L denote alloys studied by Olsen and Spanjer[1,5] for use as thermal fatigue-resistant solders.

appears in alloy K, which has the greatest amount of SbSn. The bad wetting characteristics of alloy K can also probably be ascribed to that alloy having the largest percentage of SbSn, approximately 25%. It is not surprising that alloy J was selected as being superior—in alloy J the (Sn) phase is saturated with antimony, the microstructure has 33% $Ag_3[Sn,Sb]$, which also ensures high strength, and has approximately 10% SbSn, which appears to be sufficient to ensure low ductility without having so much of this phase that wetting is adversely affected.

REFERENCES

1. D. R. Olsen and K. G. Spanjer, "Solder System," U.S. Patent 4,170,472, Oct. 9, 1979.
2. C. S. Cheng, Acta Physica Sinica, *14*, 393 (1958).
3. ASM Metals Handbook, Vol. 8, Metallography, Structures and Phase Diagrams, American Society for Metals, Metals Park, Ohio 1973.
4. F. N. Rhines, Phase Diagrams in Metallurgy, McGraw-Hill Book Co., 1956.
5. D. R. Olsen and K. G. Spanjer, Improved Cost Effectiveness and Product Reliability Through Solder Alloy Development, Solid State Technology, September, 1981, p. 121.